PROCEEDINGS, 46th Workshop on Geothermal Reservoir Engineering
Stanford University, Stanford, California, February 15-17, 2021
SGP-TR-218

Thermal-Hydrological-Mechanical Models for Evaluating Reservoir Thermal Energy Storage in the Portland Basin, Oregon

Eric L. Sonnenthal, J. Torquil Smith, Patrick F. Dobson and Peter S. Nico

Energy Geosciences Division, Lawrence Berkeley National Laboratory, 1 Cyclotron Rd. MS74R316C, Berkeley, CA 94720

elsonnenthal@lbl.gov

Keywords: reservoir-thermal-energy storage, thermal-hydrological-mechanical, numerical modeling

ABSTRACT

Several studies have explored the feasibility of Reservoir Thermal Energy Storage (RTES) in the Portland Basin, Oregon (Burns et al., 2018, 2020). Thermal-hydrological models by the latter authors have shown the effectiveness of open system heat and cold fluid storage within permeable interflow zones in the Columbia River basalts. The potential for induced or triggered seismicity and surface deformation associated with RTES has not been evaluated quantitatively in the Portland Basin, and as well as in most other RTES projects worldwide. In this study we developed a Thermal-Hydrological-Mechanical (THM) model of an idealized Portland Basin site and the simulation of a scenario similar to that explored by Burns et al. (2018). The simulation showed that thermal changes on the confined aquifer, particularly during the cooling cycle, caused near-wellbore thermal contraction and fracturing. Surface subsidence reached a maximum of about 8mm at the producing well, however alternation of injection and production in the wells could limit this effect. Given that the injection and production zones were placed at deeper levels than many areas in the Portland Basin, there is the potential for greater surface deformation locally. Changes in horizontal stresses of about 0.5 MPa extend almost a km from the wells, so the potential for triggered seismicity should be evaluated with more detailed structural models.

1. INTRODUCTION

Reservoir Thermal Energy Storage (RTES) is being evaluated in the Portland Basin, Oregon for municipal heating and cooling systems (Burns et al., 2018, 2020; Bershaw et al., 2020). Thermal-hydrological modeling by the latter authors indicated that open-loop systems drilled into permeable interflow units in buried Columbia River Basalts (CRB) would be effective for circulating/storing hot and cold water. The purpose of this study was to evaluate the potential geomechanical effects, surface deformation, and induced seismicity using Thermal-Hydrological-Mechanical (THM) modeling.

The Portland Basin is associated with several NW-SE striking faults as shown in the geologic map in Fig. 1a (Evarts et al., 2009). A schematic stratigraphic section is shown in Fig. 1b (Swanson et al, 1993).

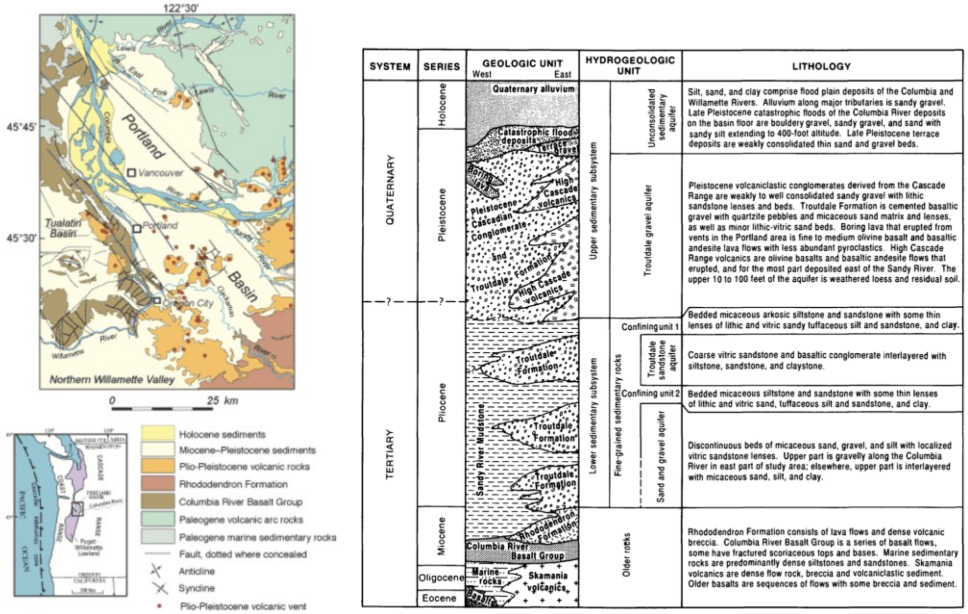

Silt, sand, and clay comprise flood plain deposits of the Columbia and Willamette Rivers. Alluvium along major tributaries is sandy gravel. Late Pleistocene catastrophic floods of the Columbia River deposits on the basin floor are bouldery gravel, sandy gravel, and sand with sandy silt extending to 400-foot altitude. Late Pleistocene terrace deposits are weakly consolidated thin sand and gravel beds.

Pleistocene volcaniclastic conglomerates derived from the Cascade Range are weakly to well consolidated sandy gravel with lithic sandstone lenses and beds. Troutdale Formation is cemented basaltic gravel with quartzite pebbles and micaceous sand matrix and lenses, as well as minor lithic-vitric sand beds. Boring lava that erupted from vents in the Portland area is fine to medium olivine basalt and basaltic andesite lava flows with less abundant pyroclastics. High Cascade Range volcanics are olivine basalts and basaltic andesite flows that erupted, and for the most part deposited east of the Sandy River. The upper 10 to 100 feet of the aquifer is weathered loess and residual soil.

Bedded micaceous arkosic siltstone and sandstone with some thin lenses of lithic and vitric sandy tuffaceous silt and sandstone, and clay.

Coarse vitric sandstone and basaltic conglomerate interlayered with siltstone, sandstone, and claystone.

Bedded micaceous siltstone and sandstone with some thin lenses of lithic and vitric sand, tuffaceous silt and sandstone, and clay.

Discontinuous beds of micaceous sand, gravel, and silt with localized vitric sandstone lenses. Upper part is gravelly along the Columbia River in east part of study area; elsewhere, upper part is interlayered with micaceous sand, silt, and clay.

Rhododendron Formation consists of lava flows and dense volcanic breccia. Columbia River Basalt Group is a series of basalt flows, some have fractured scoriaceous tops and bases. Marine sedimentary rocks are predominantly dense siltstones and sandstones. Skamania volcanics are dense flow rock, breccia and volcaniclastic sediment. Older basalts are sequences of flows with some breccia and sediment.

Figure 1. Left - Geologic Map of the Portland Basin (Evarts et al., 2009). Right – Stratigraphy of the Portland Basin (Swanson et al, 1993).

The conceptual model for RTES in the Portland Basin is shown in Fig. 2 (Burns et al., 2018). Injection into interflow units near the base of the Columbia River basalts allows for effective communication between wells and storage of heat in the underlying units primarily via conduction. The model domain explored by Burns et al. is shown in pink. To evaluate the potential for surface deformation, we extend the model to the surface (black dashed lines). Although there is significant and variable groundwater flow in the aquifers overlying the CRB, we neglect any hydraulic gradients. The interflow zones are thought to be relatively isolated, in some cases since the Pleistocene.

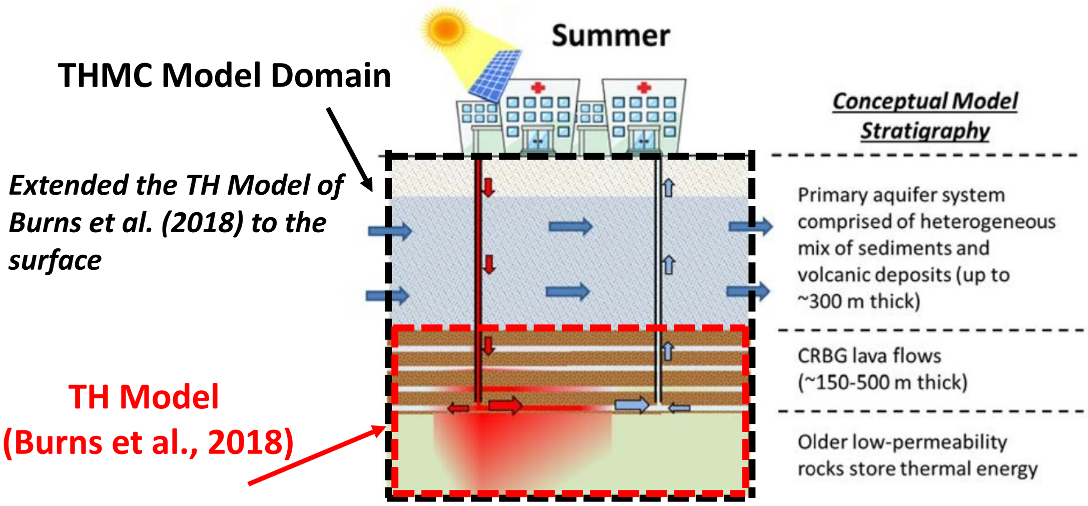

Figure 2. Conceptual model for RTES in the Portland Basin (modified from Burns et al., 2018).

2. THERMAL-HYDROLOGICAL-MECHANICAL MODELING APPROACH

THM simulations were performed using the hybrid parallel simulator TReactMech (Sonnenthal et al., 2018, 2015; Smith et al., 2015; Kim et al., 2012, 2015). Simulations included flow of water and heat (conduction and advection), thermoporoelasticity, shear and tensile failure, and tracer transport.

2.1 Numerical Grid, Initial and Boundary Conditions

The numerical grid illustrating the rock types and the location of the injection and production wells is shown in Fig. 3a. The wells are spaced approximately 500 meters apart. Fig. 3b shows the permeabilities of the rock units and the inferred initial stress state.

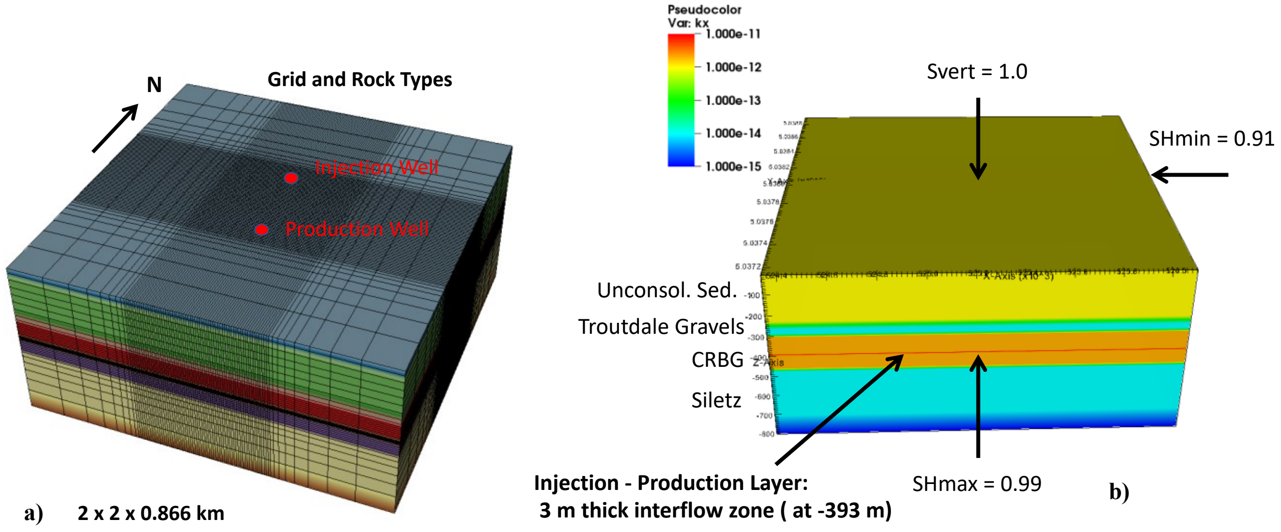

Figure 3. Left -Numerical grid, well locations, and rock types. Right – Permeabilities, relative initial stresses.

Using source mechanisms given in Yelin and Patton, 1991, and in Thomas et al. (1996), a maximum horizontal stress direction (Sh_{max}) ~ N10E was estimated, a minimum horizontal stress (Sh_{min}) of N80W, and a vertical maximum stress. Yelin and Patton (1991) suggest that the maximum and intermediate stress axes easily interchange suggesting only a small difference in stress between them. Given a 16 km depth for the magnitude 5.4 1962 Portland earthquake (epicenter actually in Vancouver, Wash.), assuming a stress drop of 10 MPa said to be typical of western N. American earthquakes and allowing 0.5 of the available difference between principal stresses to be reduced in the 1962 earthquake, suggests a 40 MPa difference in principal stresses at the depth of the 1962 earthquake. Using a generic density model from McPhee et al. (2014) gravity and aeromagnetics study of the Tualatin Basin, this implies relative stresses of 0.91:0.99:1.0 with orientations N80W:N10E:Vertical.

Hydrological and thermal properties in Table 1 are based on various sources (Burns et al., 2016, 2018; Snyder, 2008). Geomechanical properties in Table 2 were derived from Schmidt et al. (1980), Schultz (1995), and estimated.

Table 1. Preliminary Hydrological and Thermal Properties for Portland Basin

Unit	**Porosity**	**Permeability (m^2)**	**Thermal Conductivity (W/m K)^2**	**Grain Heat Capacity (J/kg/C)**	**Grain Density (kg/m^3)**
Unconsolidated Sediments	0.26 (top) 0.25	Horiz = 1 x 10^{-12} Vert = 1 x 10^{-12}	1.59	840.	2500.
Troutdale Gravels	0.28	Horiz = 1 x 10^{-12} Vert = 1 x 10^{-12}	1.59	840.	2500.
Columbia River Basalt (bulk flow)	0.02	Horiz = 2 x 10^{-12} Vert = 1 x 10^{-12}	2.50	840.	2500.
Columbia River Basalt (colonnade/entablature)	0.01	Horiz = 2 x 10^{-12} Vert = 1 x 10^{-12}	2.50	1000.	2700.
Columbia River Basalt (top)	0.10	Horiz = 1 x 10^{-11} Vert = 1 x 10^{-12}	2.50	1000.	2700.
Sediments & Volcanics	0.15	Horiz = 1 x 10^{-14} Vert = 1 x 10^{-14}	1.59	840.	2500.
Sediments & Volcanics - base	0.15	Horiz = 1 x 10^{-15} Vert = 1 x 10^{-15}	1.59	840.	2500.

Table 2. Preliminary Geomechanical Properties for Portland Basin

Unit	**Young's Modulus (GPa)**	**Shear Modulus (GPa)**	**Poisson's Ratio**	**Friction Angle (deg)**	**Dilation Angle (deg)**	**Cohesion (MPa)**	**Tensile Strength (MPa)**	**Thermal Expansion Coeff (1/°C)**
Unconsolidated Sediments	10.	4.20	0.19	35.	2.	2.	1.0	1.36 x 10^{-5}
Troutdale Gravels	10.	4.20	0.19	35.	2.	2.	1.	1.36 x 10^{-5}
Columbia River Basalt (bulk flow)	20.	7.69	0.30	37.	2.	2.	1.	6.55 x 10^{-6}
Columbia River Basalt (interior)	20.	7.69	0.30	37.	2.	2.	1.	6.55 x 10^{-6}
Columbia River Basalt (top)	20.	7.69	0.30	37.	2.	2.	1.	6.55 x 10^{-6}
Sediments & Volcanics	10.	4.20	0.19	35.	2.	2.	2.	1.36 x 10^{-5}

3. Simulation Results

Simulations were performed using maximum injection and production rates of 250 kg/s as in Burns et al. (2018), having alternating warm (32°C) and cold (5°C) water injected every 6 months for 50 years into a single well, with continuous production from the second well. Likely, most heating/cooling operations would differ from this simple case, however it is useful to look at the potential for maximum geomechanical effects using high injection rates and long periods of differing temperature injection. Fig. 4 shows the temperature distributions in the interflow unit (393 meters below the surface) during the warm injection at 49.5 years and the cold injection (50 years).

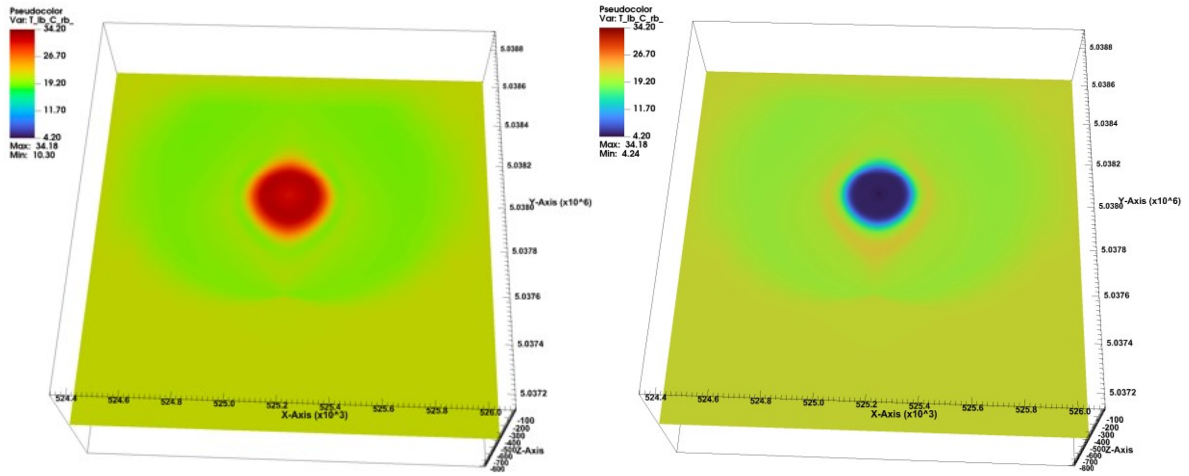

Figure 4. Temperatures at 49.5 (warm injection) and 50 years (cold injection)

Temperatures are shown at the injector and producer over time (18-50 years) in Fig. 5. Note that the temperatures are nearly stable (a very slight decline) at the producer over the entire 50 years, indicating a large region of efficient fluid mixing.

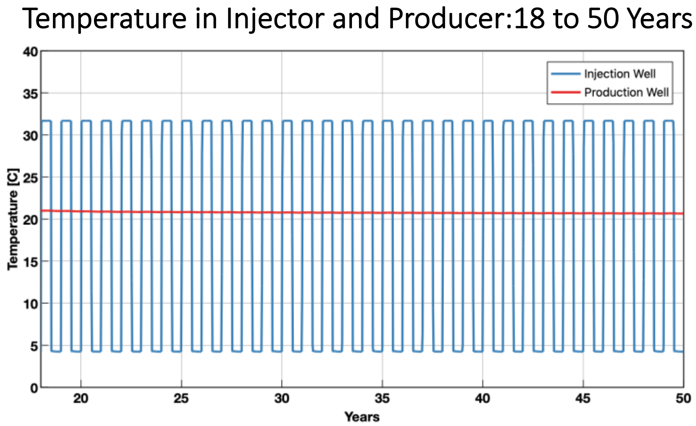

Very slight temperature decline in producer

Figure 5. Temperatures at the injector and producer from 18-50 years.

Surface deformation of a maximum of 8.5 mm after 50 years is observed at the producer (Fig. 6, left). Little deformation is observed at the injector, owing to temperature changes that cause slightly more cooling and limit uplift. Within the rock mass, a maximum vertical displacement of 11 mm (downward) at the producer and 4 mm upward at the injector is observed (Fig. 6, right). Clearly using the same wells for injection and production over the entire 50 years increases the likelihood for subsidence at the producer. Alternation of the wells (as was simulated by Burns et al., 2018) should reduce the subsidence. However, injection and production into shallower units would increase surface effects.

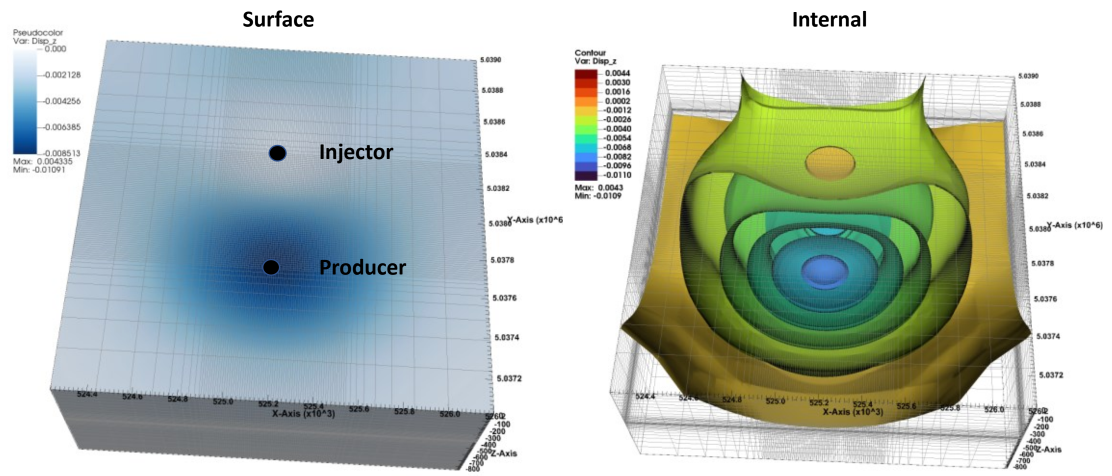

Figure 6. Left - Surface deformation at 50 years. Maximum subsidence at the producer is about 8.5 mm. Right – Vertical displacement contours, showing a maximum of about 11mm downward displacement at the producer and 4mm upward at the injector.

Horizontal (E-W) stresses (initially SHmin) are shown during the warm injection (49.5 years) and the cold injection (50 years) in Fig. 7. Significant expansion (tension) up to a km from the wells in seen during warm injection and cold injection, with local compression during cold injection. The thermal contraction associated with cold injection leads to fracturing (shear and tensile failure), beginning in the interflow unit and then migrating out of the zone over time (Fig. 8).

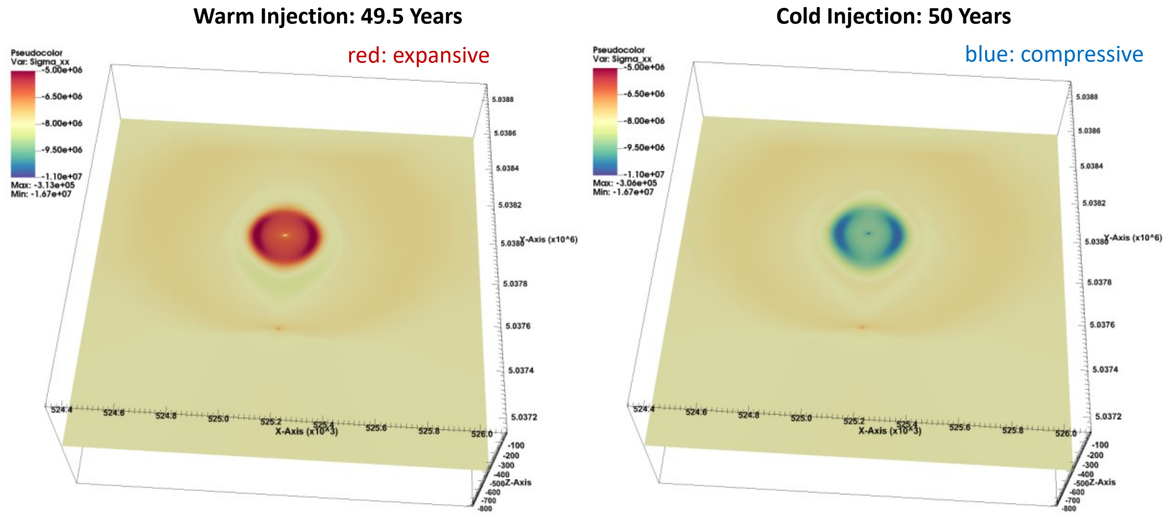

Figure 7. Left – E-W stresses at 49.5 years (warm injection). Right – E-W stresses at 50 years (cold injection).

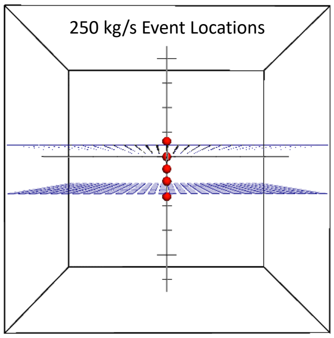

Figure 8. Shear and tensile failure locations. The horizontal planes define the 3 m thick interflow zone and the injection and production intervals.

4. CONCLUSIONS

A long-term (50 years) RTES in the Portland Basin is quite feasible with respect to thermal stability by injection into and production from interflow units in the Columbia River basalts. THM models show little thermal changes at the production well over 50 years. Subsidence at the production well (> 8 mm) is large enough to be readily observable by LIDAR and tiltmeters. However, subsidence could be mitigated by modifying injection/production wells and rates, as in some cases examined by Burns et al. (2018). During cold water injection temperature changes caused rapid contraction in the injection zone resulting in localized shear and tensile failure that propagated out of the injection zone over time. Horizontal stress changes are significant at least 500 m from the wells. Such stress changes (~0.5 MPa) are great enough to potentially result in “triggered” seismicity on faults. Therefore, any large-scale RTES in the Portland Basin should be evaluated using detailed structural models as a basis for further THM modeling.

ACKNOWLEDGMENTS

We thank Erick Burns (USGS, John Bershaw (PSU) and their team for generously sharing details of their Portland Basin study and models. This material was based upon work supported by the U.S. Department of Energy, Office of Energy Efficiency and Renewable Energy (EERE), Geothermal Technologies Office, Low-Temperature Geothermal Program, under Award Number DE-AC02-05CH11231 with LBNL.

REFERENCES

Bershaw, J., Burns, E. R., Cladouhos, T. T., Horst, A. E., van Houton, B., Hulseman, P., Kane, A., Liu, J. H., Perkins, R. B., Scanlon, D. P., Streig, A. R., Svadlenak, E. E., Uddenberg, M. W., Wells, R. E., & Williams, C. F.: An integrated feasibility study of reservoir thermal energy storage in Portland, Oregon, USA, *Proceedings*, 45th Workshop on Geothermal Reservoir Engineering, Stanford University, Stanford, California, (2020).

Burns, E. R., Bershaw, J., Williams, C. F., Wells, R., Uddenberg, M., Scanlon, D., Cladouhos, T., & van Houten, B.: Using saline or brackish aquifers as reservoirs for thermal energy storage, with example calculations for direct-use heating in the Portland Basin, Oregon, USA, *Geothermics*, **88**, (2020).

Burns, E. R., Cladouhos, T. T., Williams, C. F., & Bershaw, J.: Controls on Deep Direct-Use Thermal Energy Storage (DDU-TES) in the Portland Basin, Oregon, USA, *GRC Transactions*, **42***,* (2018).

Burns, E. R., Williams, C. F., Tolan, T., & Kaven, J. O.: Are the Columbia River Basalts, Columbia Plateau, Oregon and Washington, USA, a Viable Geothermal Target? A Preliminary Analysis, *Proceedings*, 41st Workshop on Geothermal Reservoir Engineering, Stanford University, Stanford, California, (2016).

Evarts, R. C., O’Connor, J. E., Wells, R. E., & Madin, I. P.: The Portland Basin: a (big) river runs through it, *GSA Today*, **19**, (2009), 4–10.

Kim, J., Sonnenthal, E. L., & Rutqvist, J.: Formulation and sequential numerical algorithms of coupled fluid/heat flow and geomechanics for multiple porosity materials. *International Journal for Numerical Methods in Engineering*, **92(5)**, (2012), 425–456.

Kim, J., Sonnenthal, E., & Rutqvist, J.: A sequential implicit algorithm of chemo-thermo-poro-mechanics for fractured geothermal reservoirs, *Computers & Geosciences*, **76**, (2015).

McPhee, D.K., Langenheim, V.E., Wells, R.E., & Blakely, R.J.: Tectonic evolution of the Tualatin basin, northwest Oregon, as revealed by inversion of gravity data, *Geosphere*, **10**, (2014), 264–275.

Schmidt, B. Daly, W. F., Bradley, S. W., Squire, P. R., KE/PB, and Hulstrom, L. C., Thermal and mechanical properties of Hanford basalts: compilation and analyses. RHO-BWI-C-90, Rockwell International, (1980), 214 p.

Schultz, R.A.: Limits on strength and deformation properties of jointed basaltic rock masses, *Rock Mech. Rock Eng.*, **28**, (1995) 1–15.

Smith, J. T., Sonnenthal, E. L., & Cladouhos, T.: Thermal-Hydrological-Mechanical Modelling of Shear Stimulation at Newberry Volcano, Oregon. *Proceedings of 49th US Rock Mechanics/Geomechanics Symposium of the American Rock Mechanics Association*, San Francisco, Calif., ARMA 15-0680, (2015).

Snyder, D. T.: Estimated depth to groundwater and the configuration of the water table in the Portland, Oregon area. *U.S. Geological Survey Scientific Investigations Report 2008–5059,* (2008), 40 p.

Sonnenthal, E. L., Smith, J. T., Cladouhos, T., Kim, J., & Yang, L.: Thermal-Hydrological-Mechanical-Chemical Modeling of the 2014 EGS Stimulation Experiment at Newberry Volcano, Oregon, *Proceedings*, 40th Workshop on Geothermal Reservoir Engineering, Stanford University, Stanford, California, (2015).

Sonnenthal, E., Pettitt, W., Smith, T., Riahi, A., Siler, D., Kennedy, M., Majer, E., Dobson, P., Ayling, B., Damjanac, B., and Blankenship, D.: Continuum thermal-hydrological-mechanical modeling of the Fallon FORGE site. *Geothermal Resources Council Transactions*, **42**, (2018), 1184-1193.

Swanson, R. D., McFarland, W. D., Gonthier J. B., & Wilkinson J. M.: A description of hydrogeologic units in the Portland Basin, Oregon and Washington. *U.S. Geological Survey Water-Resources Investigation Report 90-4196,* (1993), 56 p.

Thomas, G. C., Crosson, R. S., Carver, D. L., & Yelin, T. S.: The 25 March 1993 Scotts Mills, Oregon, earthquake and aftershock sequence: Spatial distribution, focal mechanisms, and the Mount Angel Fault, *Bulletin of the Seismological Society of America*, **86(4)**, (1996), 925–935.

Yelin, T. S., & Patton, H. J.: Seismotectonics of the Portland, Oregon, region, *Bulletin of the Seismological Society of America*, **81**, (1991), 109–130.